



**EUROfusion**

WP17ER-PR(18) 19457

M Vlad et al.

# **Combined effects of hidden and polarization drifts on impurity transport in tokamak plasmas**

Preprint of Paper to be submitted for publication in  
Physics of Plasmas



This work has been carried out within the framework of the EUROfusion Consortium and has received funding from the Euratom research and training programme 2014-2018 under grant agreement No 633053. The views and opinions expressed herein do not necessarily reflect those of the European Commission.

This document is intended for publication in the open literature. It is made available on the clear understanding that it may not be further circulated and extracts or references may not be published prior to publication of the original when applicable, or without the consent of the Publications Officer, EUROfusion Programme Management Unit, Culham Science Centre, Abingdon, Oxon, OX14 3DB, UK or e-mail [Publications.Officer@euro-fusion.org](mailto:Publications.Officer@euro-fusion.org)

Enquiries about Copyright and reproduction should be addressed to the Publications Officer, EUROfusion Programme Management Unit, Culham Science Centre, Abingdon, Oxon, OX14 3DB, UK or e-mail [Publications.Officer@euro-fusion.org](mailto:Publications.Officer@euro-fusion.org)

The contents of this preprint and all other EUROfusion Preprints, Reports and Conference Papers are available to view online free at <http://www.euro-fusionscipub.org>. This site has full search facilities and e-mail alert options. In the JET specific papers the diagrams contained within the PDFs on this site are hyperlinked

# ***Combined effects of hidden and polarization drifts on impurity transport in tokamak plasmas***

M. Vlad, F. Spineanu

National Institute of Laser, Plasmas and Radiation Physics, Magurele, Romania

## **Abstract**

Radial hidden drifts (HDs) of ions are generated in turbulence by a poloidal average velocity when the decorrelation time is larger than the time of flight. These drifts represent quasi-coherent motion that does not determine an average velocity but opposite displacements that compensate. We have shown that the polarization drift of the W ions determines a perturbation of this equilibrium of the HDs that generates an average radial velocity  $V_{HD}$ . The dependences of  $V_{HD}$  on plasma parameters and on the shape of the time dependence of the Eulerian correlation of the potential were studied by developing a computer code based on the decorrelation trajectory method (DTM). The pinch velocity for W ions depends on plasma rotation (L and H modes) and on the type of turbulence.

## **1. Introduction**

Tungsten is chosen as the material for plasma facing components in ITER due to its low erosion rate, low hydrogen retention and good thermal properties. The main problem is related to the large radiation of this high charge ions that can strongly affect the energy balance if they accumulate in the core plasma in concentration higher than  $10^{-4}$ . It is very important to have a correct understanding of impurity transport and to identify methods for controlling the concentration of W in tokamak core plasmas. Many experimental [1-6], theoretical [7, 8] and numerical studies [9, 10] with these goals were developed during the last twenty years. The conclusion is that the behaviour of the heavy impurities with high Z is different from that of low Z impurities. Both neoclassical and turbulence effects are shown to be important in the first case while the anomalous transport dominates in the second case [11-13]. The centrifugal force or ion-cyclotron resonance heating of minority ions can strongly influence the neoclassical transport through the generation of poloidal asymmetry. The radial convection that can have neoclassical or turbulence origins is a complex process, which can determine W-accumulation or decay.

This paper presents a theoretical analysis of the turbulent transport of heavy impurities. We show that a radial pinch velocity can be generated by the combined action of the hidden drifts (HDs) and of the polarization drift. The HDs are quasi-coherent (organized) components of ion motion in the radial direction that appear in the presence of a poloidal average velocity [14]. This motion consists of symmetrical positive and negative displacements that have zero average and do not determine a convective velocity. The polarization drift of the W ions perturbs the equilibrium of the HDs leading to radial convection. The aim of this paper is to analyse this fundamental nonlinear process and to evaluate the dependence of the pinch velocity on the parameters of the turbulence and on the poloidal velocity.

The test particle transport model is presented in Section 2 together with a review of the statistical method. Section 3 describes the new concept of HDs. The combined effects of the HDs and of the polarization drift are studied in Section 4, which also contains a general discussion of the expected

results in JET plasmas. The conclusions are summarised in Section 5.

## 2. The transport model and the statistical method

The test particle model developed in the first stage includes the ExB drift, the parallel motion, the diamagnetic velocity and the magnetic drifts. The equation for the impurity ion trajectories is

$$\frac{d\mathbf{x}}{dt} = \frac{\mathbf{E} \times \mathbf{e}_z}{B} + \frac{1}{\Omega B} \frac{\partial \mathbf{E}}{\partial t} + \mathbf{v}_m + \mathbf{V}_* + \mathbf{V}_r, \quad \frac{dz}{dt} = v_{\parallel}, \quad (1)$$

where the first term in the stochastic electric drift, the second term is the polarization drift,  $\mathbf{v}_m$  is the magnetic drift and  $\mathbf{V}_*$  is the diamagnetic velocity, which appears as an average velocity in the frame that moves with the potential, and  $\mathbf{V}_r$  is the rotation velocity. The magnetic field is along  $\mathbf{e}_z$  axis and  $\mathbf{x} = (x, y)$  is in the perpendicular plane, with  $x$  the radial and  $y$  the poloidal coordinate. We study impurity transport in the slab approximation, in the meridional plane of the plasma at the low field side. The magnetic field varies along  $\mathbf{e}_x$  axis as  $B(R) = B_0/R$ , where  $R$  is the major radius. The cyclotron frequency of the ions is  $\Omega = (Z/A)\Omega_i$ , where  $Z$  is the ionization rate of the impurities,  $A$  is their mass number and  $\Omega_i = eB/m_p$  is the cyclotron frequency of the protons. The magnetic drift is

$$\mathbf{v}_m = \frac{1}{\Omega R} (v_{\parallel}^2 + v_{\perp}^2/2) \mathbf{e}_y = \frac{2T_i(\cos^2(\theta) + 1)}{ZeBR} \mathbf{e}_y, \quad (2)$$

where  $v_{\parallel}$ ,  $v_{\perp}$  are the parallel and perpendicular components on the impurity velocity,  $\theta$  is the pitch angle of impurity velocity and  $T_i$  is the temperature of the plasma ions. Dimensionless quantities are used, with the units:  $\rho_i$  (for the distances and the correlation lengths  $\lambda_x, \lambda_y$ ), the small radius  $a$  (for the parallel distances and the correlation length  $\lambda_z$ ),  $\tau_0 = a/v_{thi}$  (for time) and the amplitude of the potential fluctuations  $\Phi$  (for the potential).  $v_{thi}$  is the thermal velocity of plasma ions. The equations (1) become

$$\begin{aligned} \frac{dx}{dt} &= K_*' \left[ -\partial_y \phi(\mathbf{x}, z, t) + C_A \partial_t \partial_x \phi(\mathbf{x}, z, t) \right] \\ \frac{dy}{dt} &= K_*' \left[ \partial_x \phi(\mathbf{x}, z, t) + C_A \partial_t \partial_y \phi(\mathbf{x}, z, t) \right] + V_t, \quad V_t = V_d + V_r + V_m, \\ \frac{dz}{dt} &= \sqrt{\frac{2}{A}}, \end{aligned} \quad (3)$$

where  $\phi(\mathbf{x}, z, t)$  is the stochastic potential of the turbulence normalised with the amplitude  $\Phi$ . They evidence five dimensionless parameters, which determine the trajectories. The parameter  $K_*'$  is the dimensionless measure of turbulence amplitude

$$K_* \equiv \frac{\Phi a}{B \rho_i^2 v_{thi}} = \frac{e \Phi a}{T_i \rho_i}. \quad (4)$$

This parameter is proportional to the Kubo number that describes the decorrelation by an average velocity  $V_*$ . The parameter of the polarization drift  $C_A$  is

$$C_A = \frac{v_{thi}}{\Omega a} = \frac{A \rho_i}{Z a}. \quad (5)$$

It depends on the mass and charge numbers ( $A$  and  $Z$ ) and on the size parameter of the plasma  $\rho_* = \rho_i / a$ .  $V_d = a / L_n$  is the normalized diamagnetic velocity, and  $V_m$  is the normalized magnetic drift

$$V_m = v_m \frac{a}{v_{thi} \rho_i} = \frac{2}{Z} \frac{a}{R} (\cos^2 \theta + 1). \quad (6)$$

The potential  $\phi(\mathbf{x}, z, t)$  is modelled as a Gaussian field with the Eulerian correlation (EC) corresponding to drift type turbulence [15-17]

$$E(\mathbf{x}, t) = \Phi^2 \partial_2 \left[ \exp \left( -\frac{x_1^2}{2\lambda_1^2} - \frac{x_2^2}{2\lambda_1^2} \right) \frac{\sin k_0 x_2}{k_0} \right]. \quad (7)$$

We have used the DTM [18, 19] for the study of this transport model. This method is based on a set of deterministic trajectories, the decorrelation trajectories (DTs), which are obtained from the EC of the potential. A set of subensembles  $S$  with given values of the stochastic functions at the origin of the trajectories  $\mathbf{x} = 0$ ,  $t = 0$

$$\phi(\mathbf{0}, 0) = \phi^0, \quad \mathbf{v}(\mathbf{0}, 0) = \mathbf{v}^0 \quad (8)$$

is defined in order to impose supplementary initial conditions to the trajectories in  $S$ .  $\mathbf{v}(\mathbf{x}, t) = -\nabla \phi(\mathbf{x}, t) \times \mathbf{e}_z$  is proportional to the ExB stochastic velocity. The potential in each subensemble  $S$  is a Gaussian field with the average

$$\Phi^S(\mathbf{x}, t) = \phi^0 E(\mathbf{x}, t) + v_x^0 \partial_y E(\mathbf{x}, t) / V_1^2 - v_y^0 \partial_x E(\mathbf{x}, t) / V_2^2 \quad (9)$$

where  $V_x = \sqrt{-\partial_y^2 E(\mathbf{0}, 0)}$  and  $V_y = \sqrt{-\partial_x^2 E(\mathbf{0}, 0)}$  are the amplitudes of the velocity components.

The subensemble average potential (9) is a function of the EC. The DTs are approximate average trajectories in the subensembles obtained by solving the equations

$$\begin{aligned} \frac{dX}{dt} &= K_* \left[ -\partial_Y \Phi^S(\mathbf{X}, Z, t) + C_A \partial_i \partial_X \Phi^S(\mathbf{X}, Z, t) \right] \\ \frac{dY}{dt} &= K_* \left[ \partial_X \Phi^S(\mathbf{X}, Z, t) + C_A \partial_i \partial_Y \Phi^S(\mathbf{X}, Z, t) \right] + V_i, \\ \frac{dZ}{dt} &= \sqrt{\frac{2}{A}}, \end{aligned} \quad (10)$$

In each  $S$ . The fluctuations of the trajectories are neglected in (10). This approximation is supported by the high degree of similarity of the trajectories in a subensemble, which occurs due to the supplementary initial conditions (8), and to the small amplitude of the velocity fluctuations in a subensemble [19].

The DTs are very simple trajectories obtained from equations (10), which have the same structure as the equations of motion (3), but with the stochastic potential replaced by the subensemble average potential (9). The DTs essentially describe the average motion inside the correlated zone during the decorrelation time  $\tau_d$ . This characteristic time is determined by the time variation of the potential and by the parallel motion.

The statistical characteristics of the stochastic trajectories are obtained by summing the contributions of all subensembles, as weighted averages of the DTs. In particular, the time dependent diffusion coefficient and the average radial displacement are

$$D_x(t) = \int d\phi^0 d\mathbf{v}^0 P(\phi^0) P(v_x^0, v_y^0) v_x^0 X^S(t), \quad (11)$$

$$\langle x(t) \rangle = \int d\phi^0 d\mathbf{v}^0 P(\phi^0) P(v_x^0, v_y^0) X^S(t), \quad (12)$$

Where  $P(v_x^0, v_y^0)$  is the probability of the initial velocity (obtained from the probability of the potential  $P(\phi^0)$ ).

The implementation of the DTM is made by a computer code that calculates a large number of DTs such that the integrals of the type (11), (12) can be evaluated with required precision. The number of DTs for the results presented in the next section is 500,000 – 1,000,000. The accuracy in the integration of equations (10) results from imposing departures smaller than 10% for 1000 rotations of the trajectories on the contour lines of the subensemble average potential in the case of static 2D turbulence. The typical run time is of the order 100 minutes.

### 3. Hidden drifts in trajectory statistics

Particle trajectories determined by the electric drift show both random and quasi-coherent aspects. The coherent motion is associated with trapping or eddying in the structure of the stochastic field. It generates quasi-coherent trajectory structures. The random motion leads to diffusive transport while the structures determine a micro-confinement process [20]. The strength of each of these aspects depends on the parameters of the turbulence. They are also strongly influenced by the presence of other components of the motion as in Eq. (1). We have shown in several studies that the transport process is completely different in the presence of structures in the sense that the dependence on the parameters is different. The quasi-coherence of the motion can also be represented by the generation of flows (that appear, for instance, due to the gradient of the confining magnetic field [17] or due the space-dependent amplitude of the turbulence).

We have show that a particular effect of the quasi-coherence appears in the presence of an average velocity  $V_t$  [14]. It is represented by the hidden drifts (HDs):

- HDs are ordered displacements that average to zero and do not drive flows
- ***HDs appear in the presence of an average velocity and they are perpendicular to this velocity***

The HDs were found by analyzing the displacements conditioned by the initial value of the potential  $\langle x(t) \rangle_{\phi_0}$ , which are evaluated in the frame of the DTM by

$$\langle x(t) \rangle_{\phi^0} = \int_{-\infty}^{\infty} dv_x^0 dv_y^0 X(t; \phi_0, v_x^0, v_y^0) P(v_x^0, v_y^0) \quad (8)$$

using the decorrelation trajectories  $X(t; \phi_0, v_x^0, v_y^0)$ , the basic concept of this method.

The conditioned displacements are zero in the case of the motion determined only by the ExB drift, but they have finite values in the presence of an average velocity  $V_t$  (as in Eq. (1)). A typical example (obtained for an isotropic static turbulence) is presented in Figure 1.a, which shows that  $\langle x(t) \rangle_{\phi_0} = 0$  at  $t=0$  and that it increases and eventually saturates. Moreover, the sign of  $\langle x(t) \rangle_{\phi_0}$  is the same as the sign of the initial potential  $\phi_0$ .

The average displacements conditioned by the sign of the potential are defined by

$$\begin{aligned} \langle x(t) \rangle_+ &= \int_0^{\infty} d\phi^0 \langle x(t) \rangle_{\phi_0} P(\phi^0), \\ \langle x(t) \rangle_- &= \int_{-\infty}^0 d\phi^0 \langle x(t) \rangle_{\phi_0} P(\phi^0) \end{aligned} \quad (9)$$

They are, as seen in Figure 1.b, time dependent functions that saturate.

The sum  $\langle x(t) \rangle_+ + \langle x(t) \rangle_- = 0$ , which shows that there is no average motion, in agreement with the constraint of the zero divergence velocity fields that states the time invariance of the distribution function of the Lagrangian velocity. In particular, the average Lagrangian velocity has to be equal to the Eulerian average velocity, which is zero along x direction (the average velocity  $V_t$  that generates the conditioned displacements is along the y direction).

The displacements  $\langle x(t) \rangle_+$ ,  $\langle x(t) \rangle_-$  depend on the average velocity represented by the parameter  $r=V_t/V$ , where  $V$  is the amplitude of the ExB stochastic velocity (see Figure 1.b).

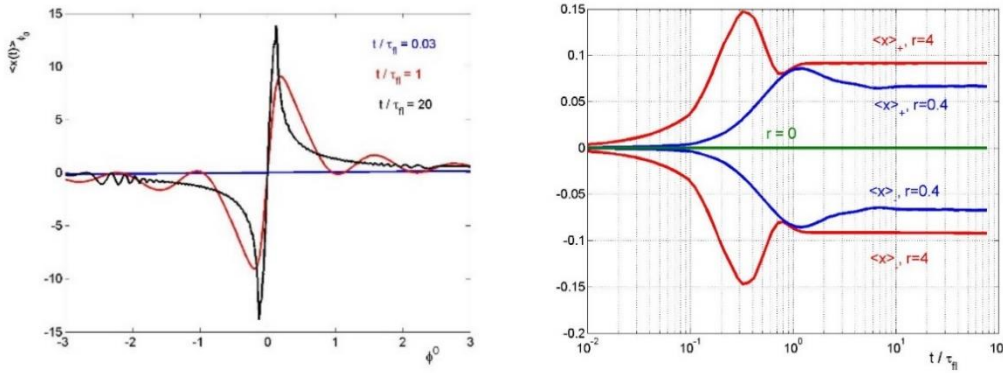


**Figure 1.** Left: the conditioned displacements  $\langle x(t) \rangle_{\phi_0}$  as functions of the initial potential;

Right: The ordered displacements as functions of time for the values of the normalized average velocity that labels the curves.

The conditioned displacements are generated also in time dependent potentials that have a finite correlation time  $\tau_c$ . They are ordered steps that appear beside the random steps (represented by the mean square displacements  $\tau_c$ ). The latter produce the diffusion of the trajectories, while the

ordered steps determine average velocities. In this case, there are conditioned average velocities, that have opposite orientations. They are determined as

$$V_{h+} = \frac{\langle x(\tau_c) \rangle_+}{\tau_c}, \quad V_{h-} = \frac{\langle x(\tau_c) \rangle_-}{\tau_c}. \quad (10)$$

They represent ordered motion that does not determine a flow since

$$V_{HD} \equiv V_{h+} + V_{h-} = 0. \quad (11)$$

These are the hidden drifts (HDs). It is interesting to note that HDs are not related to the quasi-coherent structures that can be generated in turbulence. HDs exists even if  $r > 1$  or  $\tau_c < \tau_{fl}$  when the structures are absent ( $\tau_{fl}$  is the time of flight of the trajectories over the correlation length of the potential).

The effect of the HDs on the turbulent transport is rather complex and subtle. They influence the evolution of the turbulence [14], which indirectly changes the transport. HDs appear in turbulent plasmas and they can have strong effects on the characteristics of the turbulence in the nonlinear regime when its amplitude is large. These effects essentially appear due to the correlation of the potential and density fluctuations. Such correlation does not exist for impurities, which are passively advected by the turbulence. However, we have found important effects produce by the hidden drifts in connection with the polarization drift. These direct effects corresponding to the test particle transport are essentially determined by the perturbation of the equilibrium between the positive  $V_{h+}$  and the negative  $V_{h-}$  drift, which is produced by the polarization drift.

#### 4. Combined effects of the hidden and polarization drifts on impurity transport

The transport model (1)-(7) was studied using the DTM.

We have found that the polarization drift determines significant modifications of the HDs. We present three typical cases with and without polarization drift and with two type of time dependence of the correlation of the potential. As the polarization drift contains the time derivative of the stochastic electric field, it is expected that the influence is not only determined by the decorrelation time  $\tau_d$ , but by details of the function  $E(t)$ . We have considered an exponential decay and an oscillating decay. The cases presented in Figures 1-5 are:

- (a) exponentially decaying  $E(t)$  without polarization drift ( $C_A=0$ ),
- (b) exponentially decaying  $E(t)$  and polarization drift with  $C_A=0.2$ ,
- (c) oscillating  $E(t)$  and polarization drift with  $C_A=0.2$ .

One can see in Figure 2 the conditioned displacements for the three cases.

- (a): The conditioned displacements are anti-symmetrical functions of the initial potential at any time when the polarization drift is zero. The HDs are symmetrical and the average velocity  $V_{HD}$  is zero.
- (b): The presence of the polarization drift perturbs the symmetry of the displacements at large times by increasing the positive displacements and decreasing the negative ones. This leads to a finite positive average velocity  $V_{HD}$ .
- (c): The perturbation of the symmetry of the conditioned displacements is much stronger for the



oscillatory decay of  $E(t)$ . It leads to the reversal of the sign of the displacements for positive initial potential at large time.

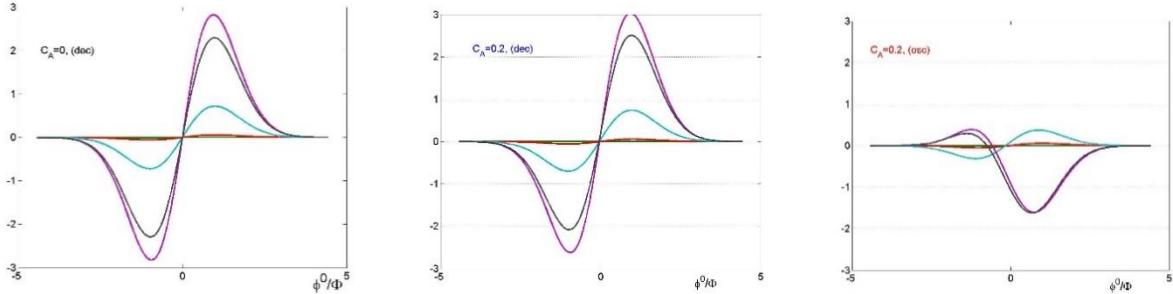


**Figure 2.** The conditioned displacements  $\langle x(t) \rangle_{\phi_0} P(\phi^0)$  as functions of the initial potential for  $t=0.4$  (green), 1.6 (red), 6 (cyan), 23 (magenta), 76 (black) for (a) exponential EC without polarization drift, (b) exponential EC with polarization drift and (c) oscillating EC with polarization drift.

This behaviour can also be seen in Figure 3 where the ordered displacements obtained from the results of Figure 2 are shown. It clearly appears that the polarization drift destroys the symmetry of the ordered displacements and that this process is much more efficient for oscillating  $E(t)$  than for exponential  $E(t)$ .

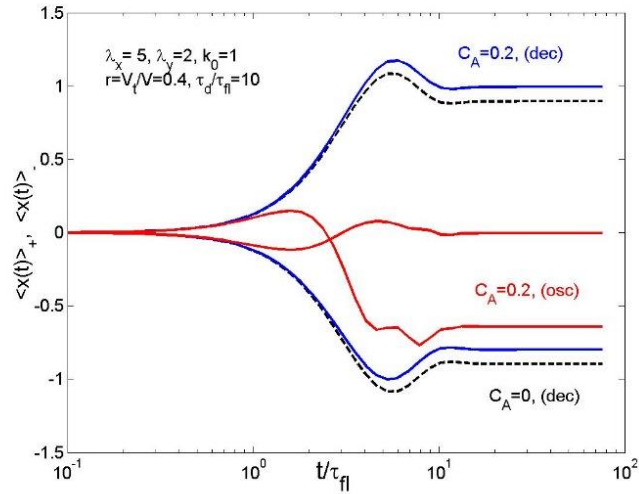


**Figure 3.** The ordered displacements as functions of time for the three cases presented in Figure 2: (a) dashed black lines, (b) blue lines and (c) red lines.

The average velocity generated from the combined action of the HDs and polarization drift for the three cases is shown in Figure 4. The direct transport is much larger for the oscillating EC and its velocity  $V_{HD}$  becomes negative. The largest radial velocity appears in the case of oscillating EC, besides the small HDs seen in Figure 2c. The cause of this behaviour is the large perturbation of the HDs produced by the polarization drift in the case (c).

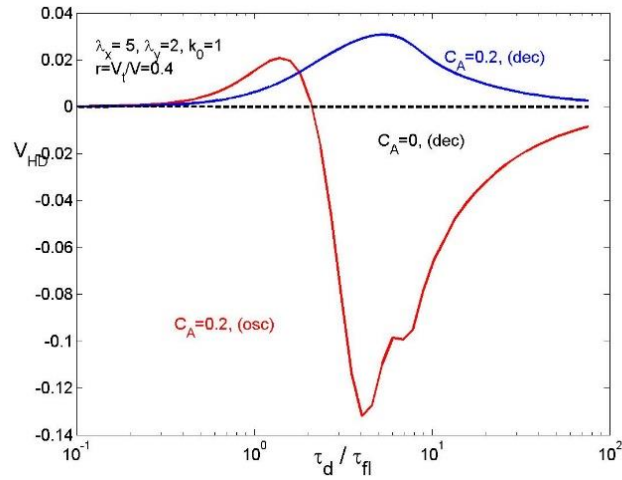


**Figure 4.** The average velocity determined by the HDs for the three cases presented in Figure 2: (a) dashed black line, (b) blue line and (c) red line.

The strongest influence that is produced by oscillating potentials is observed also in the diffusion coefficient. Figure 5 shows that  $D_x$  is unchanged by the polarization drift in the case of exponentially decaying  $E(t)$  (case (b) is superposed on case (a)) and that the asymptotic value of the diffusion coefficient increases significantly in case (c).

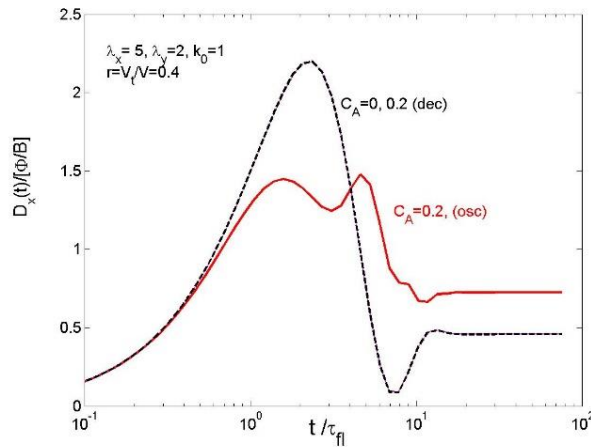


**Figure 5.** The diffusion coefficient for the three cases presented in Figure 2: (a) and (b) dashed black line, (c) red line.

Thus, the interaction of the HDs with the polarization drift determines an average velocity (direct transport) in the radial direction (perpendicular to the average velocity  $V_t$ ). The velocity  $V_{HD}$  has a complicated dependence on the parameters of the turbulence, on the average velocity in Eqs. (1) and on the shape of the time correlation of the potential.

The transport depends on the total velocity  $V_t$ . However, it is important to consider the components determined by different processes (magnetic drift  $V_m$ , diamagnetic velocity  $V_d$  and plasma rotation  $V_r$ ) because they depend on different parameters and can have different signs.

The mass dependent terms in Eqs. (1) are the polarization drift and in the parallel motion. The strongest dependence on  $A$  is produced by the parallel velocity. The polarization drift remains much smaller than the ExB drift, even with the increase given by the factor  $A/Z$ . It is thus not expected to bring strong  $A$  dependent effects.

The main difference between the heavy and light impurities is the parallel decorrelation time which is much larger in the first case. The parallel decorrelation time is very large for W ions, which determines strong difference of the diffusion coefficient  $D_x$  compared to the plasma ion  $D_0$  (see [15]). We have found  $D_x / D_0 \approx 1/A^\gamma$  where the power  $\gamma$  is  $\gamma = 1/2$  in the case of quasi-linear regime and  $\gamma < 1/2$  for the nonlinear regime, with values that depend on the space dependence of the EC of the potential. These results were obtained for decaying time dependence of the turbulence. In the case of time oscillating  $EC(t)$ , the dependence of  $D_x$  and  $V_{HD}$  on the parameters is complex and simple transport regimes cannot be deduced from the results.

The dependence of the heavy impurity transport on the velocity  $V_t$  was studied in the frame of the complete model (1)-(7). We have shown that the radial velocity  $V_{HD}$  produced by the HDs and the polarization drifts has a nontrivial dependence on  $V_t$ .

Figure 7 presents the result obtained for the W impurities in the case of oscillating  $EC(t)$ , for the parameters  $K_*' = 10, \lambda_x = 5, \lambda_y = 2, k_0 = 1, \tau_z = 10$ . One can see that in the absence of the hidden drifts (at  $V_t=0$ ), the radial velocity is zero,  $V_{HD}$  changes the sign when  $V_t$  changes the sign (it is anti-symmetrical in  $V_t$ ) and that it is negative at  $0 < V_t < 2$  and positive at larger  $V_t$ .

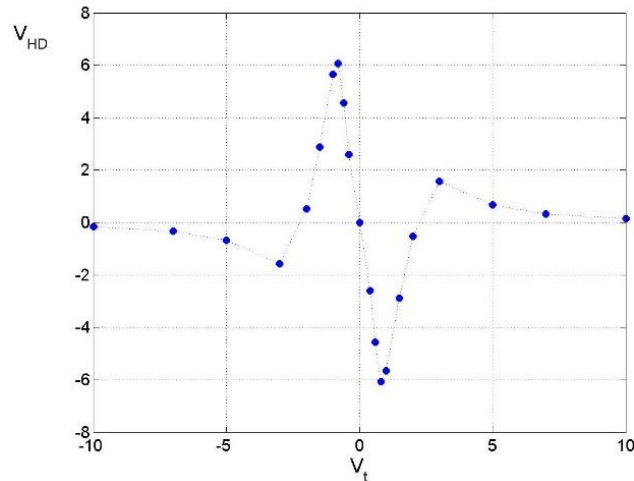


**Figure 6.** The radial drift velocity determined by the combined effect of the HDs and of the polarization drift as function of the poloidal average velocity. Both velocities are normalized with the diamagnetic velocity  $V_* = \rho_i v_T / a$ .

The contribution of the magnetic drifts to the total poloidal velocity  $V_t$  is negligible for the W impurities (due to their charge that is of the order 10, the normalized  $V_m$  is of the order 0.1).

The experiments on JET [21] have obtained in the L mode negative values of the radial electric field of the order of few kV/m and, in the H mode, positive electric fields of few tens of kV/m. These are value estimated from the measurements at  $\rho=0.75$  in the results presented in [21].

The normalized diamagnetic velocity is of the order of units  $V_d \sim 3$ . It is positive for the ITG turbulence and negative for the TEM and drift turbulence.

Thus, in the L mode, the total poloidal velocity  $V_t$  is of the order 4 in the case of ITG turbulence and it is around -2 for TEM. According to Figure 7, the average velocity  $V_{HD}$  contributes to impurity removal in ITG turbulence, while in the case TEM the pinch is in the region of transition between positive and negative values. In H modes,  $V_t$  is around zero for the ITG and around -7 for TEM turbulence. Figure 7 suggests that a rather large pinch can appear in the ITG turbulence, which are directed inward or outward (depending on the specific values of the parameters). In the case of TEM turbulence the pinch is inward, but with small velocity.

## 5. Conclusion

Radial drifts of ions are generated in turbulence by a poloidal average velocity when the decorrelation time (produced by the parallel motion or by the time variation of the potential) is larger than the time of flight. These drifts that we have named **hidden drifts** (HDs) represent quasi-coherent motion that does not determine an average velocity but opposite displacements that compensate. However, the HDs represent a reservoir of radial pinch, because any perturbation of the exact equilibrium of the positive and negative organized motion leads to radial pinch.

We have shown that the polarization drift of the W ions provides such perturbation of the equilibrium of the HDs, which generates an average radial velocity  $V_{HD}$ . The dependence of this velocity on plasma parameters is rather complex. Moreover,  $V_{HD}$  is influenced by the shape of the time dependence of the Eulerian correlation of the potential. Much stronger effects appear in the case of oscillating  $E(t)$  compared to exponentially decaying  $E(t)$ .

This analysis permitted to draw the physical explanation for the direct transport (average velocity) found in the presence of an average poloidal velocity when the polarization drift is large enough. The dependence of the average velocity  $V_{HD}$  on the poloidal velocity  $V_t$  is nontrivial, with several changes of the direction. This leads to different behaviours in the L and H modes and also to differences between ITG and TEM turbulence. Our present estimations for the ITG turbulence predict an outward pinch in the L mode and much larger pinches directed inward or outward (depending on the specific values of the parameters) in the H mode.

## Acknowledgement

This work has been carried out within the framework of the EUROfusion Consortium and has received funding from the Euratom research and training programme 2014-2018 under grant agreement No 633053 and also from the Romanian National Education Minister under contract 2/23.02.2016. The reviews and opinion expressed herein do not necessarily reflect those of the European Commission.

## References

- [1] Pütterich T., et al., Plasma Phys. Control. Fusion 55, 124036 (2013).
- [2] Neu R. et al., J. Nucl. Mater. 313–316, 116 (2003).

- [3] Dux R. et al., Plasma Phys. Control. Fusion 45, 1815 (2003).
- [4] Sertoli M. et al., Plasma Phys. Control. Fusion 53, 035024 (2011).
- [5] Puiatti M. et al., Phys. Plasmas 13, 042501 (2006).
- [6] Valisa M. et al., Nucl. Fusion 51, 033002 (2011).
- [7] Angioni C. and Helander P., Plasma Phys. Control. Fusion 56, 124001 (2014).
- [8] Moradi S., Fülöp T., Mollén A. and Pusztai I., Plasma Phys. Control. Fusion 53, 115008 (2011).
- [9] Casson F. J. et al., Plasma Phys. Control. Fusion 57, 014031 (2015).
- [10] Guirlet R. et al., Plasma Phys. Control. Fusion 48 B63 (2006).
- [11] Valisa M. et al and JET-EFDA contributors Nucl. Fusion 51 033002 (2011)
- [12] Casson F. J. et al., Nucl. Fusion 53, 063026 (2013).
- [13] Yamoto S. et al., Nucl. Fusion 57, 116051 (2017).
- [14] Vlad M., Spineanu F., Hidden drifts in turbulence, JET pinboard, to be submitted for publication.
- [15] Vlad M., Spineanu F., Phys. Plasmas 20, 122304 (2013).
- [16] Vlad M., Spineanu F., Phys. Plasmas 22, 112305 (2015).
- [17] Vlad M., Spineanu F., Nuclear Fusion 56, 092003 (2016).
- [18] Vlad M., Spineanu F., Misguich J. H., Balescu R., Phys. Rev. E 58, 7359 (1998).
- [19] Vlad M., Spineanu F., Phys. Rev. E 70, 056304 (2004).
- [20] Vlad M, Spineanu F, Focus on Turbulence in Astrophysical and Laboratory Plasmas, New Journal of Physics 19 (2017) 025014.
- [21] Andrew Y., et al., EPL 83 15003 (2008).
- [22] Vlad M., Spineanu F., Benkadda S., Physical Reviews Letters 96, 085001 (2006).